THE ASTROPHYSICAL JOURNAL, 409:L1–L4, 1993 May 20

MEASUREMENTS OF THE ANISOTROPY OF THE COSMIC BACKGROUND RADIATION AT 0°.5 SCALE NEAR THE STAR μ PEGASI

P. MEINHOLD,[1] A. CLAPP,[2] M. DEVLIN,[2] M. FISCHER,[2] J. GUNDERSEN,[1] W. HOLMES,[2] A. LANGE,[2]
P. LUBIN,[1] P. RICHARDS[2], AND G. SMOOT[3]
Received 1993 January 8; accepted 1993 March 3

ABSTRACT

Results are presented from the third flight of the MAX experiment, an attitude-controlled balloon-borne millimeter-wave telescope with a 0°.5 beam, a 1° chop, and a three-channel bolometric photometer. Several hours of high-quality data were obtained during a flight on 1991 June 5, including long integrations to search for CBR anisotropy, two separate measurements of dust in the Galactic plane, a brief scan of the Coma Cluster to search for the Sunyaev-Zel'dovich (SZ) effect, and a number of important systematic tests. Data from one of the long CBR integrations, carried out in a region of sky near the star Mu Pegasi, are presented. The primary structure in the data is shown to be emission from Galactic dust via its spectrum and correlation with the *IRAS* 100 μm map. Several approaches are used to fit this dust component and remove it from the data. An upper limit to CBR anisotropy of $\Delta T/T < 2.5 \times 10^{-5}$ is obtained for a Gaussian autocorrelation function with coherence angle $\theta_c = 25'$. This limit is significantly higher than the measurement sensitivity of $\Delta T/T \approx 1 \times 10^{-5}$ due to the presence of residual structure in the data after removal of the dust component.

Subject headings: cosmic microwave background — dark matter — large-scale structure of universe

1. INTRODUCTION

Measurements of the anisotropy of the cosmic background radiation (CBR) are effective and useful tools for testing cosmological models. Such measurements constrain the initial conditions from which large-scale structure in the universe may have formed. Measurements on intermediate angular scales (0°.5 to several degrees) are also sensitive to the details of structure formation and to the ionization history of the universe for $z < 1000$. Recent limits on small and medium angular scales (Readhead et al. 1989; Meinhold & Lubin 1991; Gaier et al. 1992) have constrained the allowed values of the biasing parameter in CDM (cold dark matter) models (Bond et al. 1991; Vittorio et al. 1991). More powerful tests of cosmological models are possible when these measurements are combined with measurements from the *COBE* (*Cosmic Background Explorer*) satellite (Smoot et al. 1992) at large angular scale, as well as other measurements of large-scale structure in the universe.

Measurements made on a scale relevant to CDM models, with substantially increased sensitivity on half-degree scales, are described. It is expected that these results will have a significant impact on the parameter space available to CDM models. These models will be critically tested by modest improvements in CBR anisotropy measurements at intermediate angular scales.

2. THE EXPERIMENT

The instrument used for the millimeter wave anisotropy experiment (MAX) has been described in detail in previous work (Fischer et al. 1992; Alsop et al. 1992; Meinhold et al. 1993, hereafter collectively FAM). It consists of a 1 m off-axis Gregorian telescope with secondary mirror modulation feeding a ^{3}He-cooled bolometric photometer, all mounted on a balloon-borne attitude-controlled platform. The photometer has passbands centered at 6, 9, and 12 cm^{-1} (180, 270, and 360 GHz) with 30%–40% bandwidths. The bands were chosen to minimize atmospheric emission and to provide the spectral discrimination required to separate the CBR anisotropy signal from emission from cool (≤ 20 K) galactic dust.

The 6, 9, and 12 cm^{-1} filters respectively have effective band centers of 181, 270, and 381 GHz for $\Delta T/T$ of a 2.74 K Planck spectrum, 195, 290, and 408 GHz for a Rayleigh-Jeans emitter, and 218, 305, and 417 GHz for an 18 K dust emitter with emissivity proportional to $\nu^{1.4}$. These bands also measure above and below the crossover of the SZ spectral distortion (Sunyaev & Zel'dovich 1972). The optics are designed to produce a beam on the sky which is nearly Gaussian with full width at half-maximum (FWHM) response of approximately 30′ in all three bands. The secondary mirror of the telescope nutates sinusoidally at 6 Hz to throw the beam $\pm 0°.65$ on the sky. The detector output is demodulated using the secondary position as a reference. This produces what is normally referred to as a single-chop response which is well approximated by two Gaussians of FWHM = 36′ and a separation of 1°. For detailed descriptions of this as well as details of photometer design, sidelobe response, pointing performance, calibration procedures, and performance on previous flights, refer to FAM.

A number of improvements were made to the system before the third flight in 1991 June. New bolometric detectors were installed, with higher sensitivity, and additional low-pass filters were added to reduce high-frequency leakage. Radio frequency (RF) filters were installed on the bolometer leads by casting them into Eccosorb^{tm} epoxy, in a successful attempt to reduce system sensitivity to terrestrial radio interference, which was a problem in the second flight in 1990 July. A "blank" or non-optical bolometer was maintained without an RF filter as an RF sensor. Although sensitivity to terrestrial RF was reduced, strongly directional RF interference was noted during the

[1] Physics Department, University of California at Santa Barbara, Santa Barbara, CA 93106; also NSF Center for Particle Astrophysics.
[2] Physics Department, University of California at Berkeley, Berkeley, CA 94702; also NSF Center for Particle Astrophysics.
[3] Physics Department, Lawrence Berkeley Laboratory, Berkeley, CA 94720; also NSF Center for Particle Astrophysics.

flight, and limited target selection for the long CBR anisotropy integrations. An intensified CCD camera with an adjustable zoom lens was added to aid in telescope pointing. An improvement in sensitivity for star tracking from 4.5 to about 9.5 mag was demonstrated early in the flight.

The telescope with nutating secondary makes a first difference measurement (ΔT) for each orientation of the platform. For long CBR integrations, the platform was slewed smoothly in azimuth from $+3°$ to $-3°$ on the sky relative to a chosen fiducial tracking point (usually a star). This slew is referred to as a "half scan," with a "full scan" extending from $+3°$ to $-3°$ to $+3°$. The platform stopped once during each full scan for 10 s to adjust pointing and completed one full scan every 108 s. This is almost 3 times faster than the scan rate used for the earlier measurements, and the increased speed reduced susceptibility to long-term drifts in the instrument and the atmosphere.

The third flight of MAX took place 1991 June 5–6 from the National Scientific Ballooning Facility (NSBF) in Palestine, Texas. Roughly 10 hr at a float altitude of about 35.4 km were obtained, using a 3.1×10^5 m^3 helium-filled balloon. The experiment was flown roughly 4.6 km higher than the two previous flights to reduce long-term drifts in the data due to atmospheric emission. Two deep integrations to search for CBR anisotropy were performed, in addition to a number of other tests and measurements.

3. THE MEASUREMENT

The first CBR integration was carried out in a dark region of the sky near the star Gamma Ursae Minoris. These results will be reported in a separate publication (Gundersen et al. 1993). The deep CBR integration discussed here was carried out around the star Mu Pegasi ($\alpha = 22^h50^m$, $\delta = 24°33'$, epoch 1991). The target was chosen to be nearly due east at the start of the measurement so that there would be little rotation of the measured strip relative to constant celestial coordinates for the duration of the integration. This target was a compromise between moderately low dust emission, the availability of guide stars, and the absence of excessive RF interference. Other regions exist where the anisotropic dust emission is smaller by a significant factor (≈ 10), as measured by *IRAS* at 100 μm. In particular, the region of the star Gamma Ursae Minoris, mentioned above, has roughly a factor of 5 less anisotropic emission.

The integration lasted from 8.3 to 9.8 UT. A calibration was performed at 9.1 UT using a membrane transfer standard, as described in Fischer et al. (1992). Forty-six full scans of the region were made, for a total integration time of 1.4 hr. This data set is free of serious RF interference (as measured by the correlations between the optical bolometer channels and the blank "RF" channel) and shows only a small level of excess $1/f$ noise on long time scales. Transients in the bolometer signals due to cosmic-ray events were removed from the data as described in Alsop et al. (1992). This process removed about 10% of the data, with an average rate of 10 events per bolometer per minute. The data were phase-synchronously demodulated using the secondary mirror position as a reference, and long-term offset drifts were reduced by removing an offset for each full scan. After this fitting, the data were binned into 21 positions. The number of bins used must be taken into account in calculating sensitivity for a given sky model. The 1 s noise per channel, as measured over 100 s, gives effective 1 s sensitivities of 0.22, 0.13, and 0.1 mK to a Rayleigh-Jeans source in the 6, 9, and 12 cm^{-1} channels, respectively. This sensitivity translates to 0.51, 0.73, and 2.25 mK s$^{1/2}$ when referred to a 2.74 K blackbody. These numbers are consistent with the sensitivities expected based on preflight tests. The effective integration time for most of the bins after cosmic ray removal and editing is about 220 s and more than twice this for the center point of the scan.

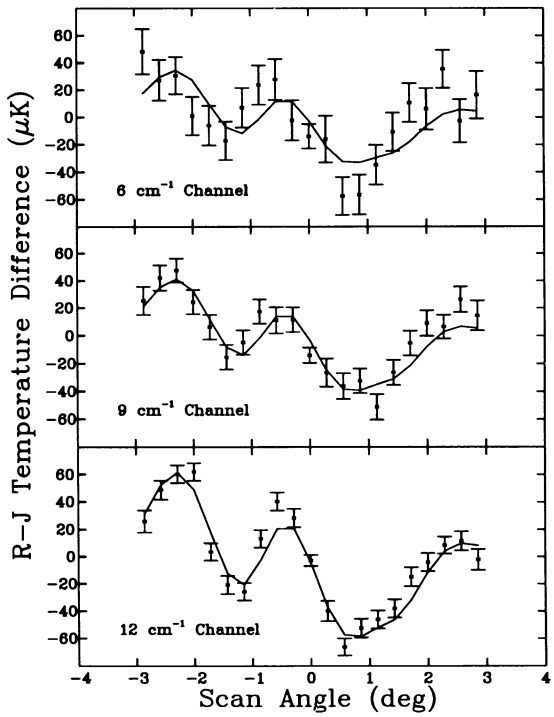

FIG. 1.—Binned data from deep integration near Mu Pegasi. Vertical axis is Rayleigh-Jeans temperature difference, and error bars are ± 1 σ. Solid lines are scaled from *IRAS* 100 μm map.

The resulting data sets are shown in Figure 1 and Table 1. Note that the calibrations are in antenna temperature differ-

TABLE 1

BINNED DATA FROM DEEP INTEGRATION NEAR MU PEGASII

Bin	6 cm^{-1}	9 cm^{-1}	12 cm^{-1}
−2.857	48.4 ± 16.5	25.4 ± 10.3	26.0 ± 8.1
−2.571	27.4 ± 15.0	42.2 ± 9.3	48.7 ± 6.9
−2.286	30.8 ± 13.7	47.7 ± 8.7	60.3 ± 6.5
−2.000	1.1 ± 14.0	24.4 ± 8.9	61.9 ± 6.4
−1.714	−5.9 ± 14.5	6.3 ± 8.9	3.6 ± 6.4
−1.429	−17.0 ± 14.0	−15.3 ± 8.9	−20.7 ± 6.6
−1.143	7.2 ± 14.5	−4.8 ± 8.8	−25.7 ± 6.5
−0.857	23.8 ± 14.4	17.5 ± 8.7	13.3 ± 6.4
−0.286	27.9 ± 15.0	11.2 ± 9.5	40.4 ± 6.5
0.000	−2.1 ± 14.7	11.6 ± 8.9	28.5 ± 6.7
0.286	−13.7 ± 8.9	−13.9 ± 5.5	−2.8 ± 4.1
0.571	−15.8 ± 17.1	−26.4 ± 10.2	−39.8 ± 7.4
0.857	−57.4 ± 13.9	−36.2 ± 9.3	−66.1 ± 6.2
1.143	−56.5 ± 14.6	−32.4 ± 8.8	−52.4 ± 6.9
1.429	−34.6 ± 14.5	−51.2 ± 9.1	−46.1 ± 6.6
1.714	−10.6 ± 14.0	−26.4 ± 9.0	−38.0 ± 6.7
2.000	10.7 ± 14.2	−5.3 ± 8.7	−14.9 ± 6.9
2.286	6.1 ± 15.2	9.0 ± 9.2	−4.1 ± 6.7
2.571	35.6 ± 14.0	6.4 ± 8.5	8.4 ± 6.3
2.857	−2.7 ± 15.8	26.3 ± 9.3	11.6 ± 7.1
	16.5 ± 17.4	14.5 ± 10.8	−2.1 ± 7.7

NOTE.—Rayleigh-Jeans temperature differences in μK.

ences, for simpler comparison with foreground models. To scale the 6, 9, and 12 cm^{-1} data relative to a 2.74 K blackbody, multiply by 2.3, 5.6, and 20.5, respectively. The solid lines on the plots are discussed below. The average error bars are 14.5, 8.9, and 6.6 μK T_a in the 6, 9 and 12 cm^{-1} data sets, respectively. Comparison of these error bars with the short-term noise described above shows that the noise is decreased by averaging as expected for an ideal random (Gaussian distributed) variable.

4. SPECTRAL ANALYSIS AND FOREGROUND SUBTRACTION

The large correlated signal seen in all three channels has a rising spectrum relative to Rayleigh-Jeans. The most likely candidate to explain this structure is emission from interstellar dust (ISD) in our Galaxy. To analyze the data in terms of CBR anisotropy, this ISD must be removed, using its spectrum and possibly its morphology. The data have been analyzed in three distinct ways: subtraction of a fit to the ISD emission as measured by the *IRAS* satellite at 100 μm; subtraction of an ISD component obtained from an internal fit to all three channels; simultaneous two-component analysis of the data in terms of ISD emission and some other component such as CBR fluctuations, synchrotron emission etc. Each of these methods gives a similar result for upper limits to CBR fluctuations with Gaussian autocorrelation function (ACF).

The solid lines included in Figure 1 show the fit of the *IRAS* data to the present measurements. A 100 μm map with 1′ pixels obtained from IPAC was convolved with a 0°.5 FWHM Gaussian, chopped sinusoidally with 0°.65 amplitude, and sampled along the lines of sight observed during the measurement. The *IRAS* differences were binned in the same way as the flight data, and the amplitude was scaled to fit each of the three MAX channels. There is an extremely good correlation between the *IRAS* data and these measurements, leaving little doubt that most of the measured structure is due to ISD emission. We model the dust using the ratios of the structure measured in the three channels to that measured at 100 μm, and the simplistic assumption that the dust varies as $B = A\nu^{\alpha}B_{\nu}(T_d)$. Here, $B_{\nu}(T_d)$ is the Planck function, $A\nu^{\alpha}$ is an emissivity, and ν is in Hz. An emissivity index of $\alpha = 1.4$ and a temperature of 18 K are found. The parameter A has an rms of $\approx 2 \times 10^{-20}$. When this best-fit dust component is subtracted, the total χ^2 of the residuals is 108.5 for 57 degrees of freedom.

The second method of analysis is a "single-component" internal fit to find a model of arbitrary morphology and spectrum which minimizes the χ^2 of the residuals. The resulting best-fit spectrum is not well parameterized by a simple dust model, but is marginally consistent with the $T = 18$ K, $\alpha = 1.4$ dust found from the first method. The residuals from this fit have a total χ^2 of 53.5 for 38 degrees of freedom, with a probability for exceeding this χ^2 filter leakage. Measurements made before the flight placed a limit of 1% on the integrated response of the system above 25 cm^{-1}. If this response peaked at the worst possible frequency, the true value of α could be as high as 1.65.

For both of these approaches, the residual signal or "second component" has significant structure and may be due to any of the following: emission from extragalactic sources; synchrotron or bremsstrahlung emission from the galaxy; errors in dust subtraction; multiple interstellar dust components (or variations in spectral index); residual atmospheric emission; telescope far sidelobe response; unknown systematic errors in the experiment; or CBR anisotropy.

Under the assumption that there is signal from some component other than the ISD in the data, the appropriate method of signal analysis is a two-component internal fit. The data are simultaneously fitted to two components of arbitrary morphology, each with a particular spectrum. In general, the fits produce one component which is spectrally and morphologically like the *IRAS* 100 μm dust, and a "second component," possibly independent of the dust. The second component signal varies in both shape and spectrum depending on the choice of fitting parameters and on the details of the data reduction. In particular, the exact details of the binning strategy affect the results. The results of a few of these fits are summarized in Table 2 along with results of the first two subtraction methods. A preliminary report of fits to these data was given by Devlin et al. (1992), including a plot of the residuals from one particular CBR fit as a function of sky position. Since the morphology of the residual is sensitive to the way in which the fit is done, it is not reproduced here. Although it is not possible to distinguish between possible sources of the second component from the quality of the fits, not all of the possibilities are equally likely. Arguments given in Alsop et al. (1992), based on standard models for diffuse synchrotron and bremsstrahlung emission from our Galaxy, suggest that these sources are unlikely to contribute significantly in our relatively high frequency bands. The correlation coefficients given in

TABLE 2

SUMMARY OF RESULTS OF TWO-COMPONENT FITTING

Second Component	Residual χ^2	DF[a]	Probability[b]	RMS[c] (μK)	100 μm Correlation[d]	First-Component Correlation
Bremsstrahlung[e]	19.1	18	38%	20	0.29	0.18
Synchrotron[f]	19.9–20.3	18	34%–32%	20	0.31	0.25
2.735 K Planck (CBR)	18.7	18	41%	19	0.29	0.22
Rayleigh-Jeans	19.7	18	39%	26	0.26	−0.47

NOTE.—Two components of arbitrary morphology and fixed spectra have been simultaneously fitted to the data. The first component in all cases has been constrained to be dust with a temperature of 18 K and a spectral index $\alpha = 1.4$.

[a] Degrees of freedom are found from (number of data points) − (fitting parameters), or 3 × (number of bins − 3(for offset subtraction) − 2 × (number of independent points per component) − 2(spectral fitting parameters).

[b] Probability of exceeding the residual χ^2 for the specified number of degrees of freedom for random data.

[c] RMS of the "second component" of the two-component model, where the "first component" is one with a dust spectrum. The RMS is given in Rayleigh-Jeans units, normalized to 6 cm^{-1}.

[d] Correlation coefficient calculated between the *IRAS* 100 μm data and the second component of the model.

[e] A spectral index of −2.1 has been used for bremsstrahlung.

[f] Spectral indices of −2.7 and −3.1 have been used for synchrotron radiation.

Table 2 also help to distinguish reasonable models for the second component, in that the two components are not expected to be significantly correlated.

Since these data do not uniquely determine the shape or spectrum of the "second component" or residual signal, they have been analyzed in terms of an upper limit to CBR anisotropy only. This does not rule out the possibility that some or all of the residual signal is due to CBR fluctuations. Upper limits are calculated in the next section using the 2.74 K Planck spectrum (CBR) fit component. This is the most conservative choice for calculating an upper limit, since it assumes that all of the structure not associated with ISD emission is CBR anisotropy.

5. INTERPRETATION

Upper limits to intrinsic sky fluctuations with a Gaussian autocorrelation function (ACF) are calculated for comparison to theory and to other measurements:

$$C(\alpha, \sigma_b, \phi_c) \equiv C_0 \frac{\phi_c^2}{2\sigma_b^2 + \phi_c^2} \exp\left[-\frac{\alpha^2}{2(2\sigma_b^2 + \phi_c^2)}\right]. \quad (1)$$

Here a Gaussian beam response of dispersion σ_b has been convolved with a Gaussian ACF of coherence angle ϕ_c and intrinsic amplitude C_0, sampled at points separated by an angle α. Assuming this effective ACF, a likelihood function for the data is calculated including all the bin-to-bin correlations from the theoretical correlation function based on the chop and scan strategy (with a square wave chop approximation).

A Bayesian method assuming a uniform prior likelihood distribution has been used to calculate upper limits to this ACF from the likelihood function. The 95% confidence level upper limit derived this way is $\Delta T/T < 5.3$, 3.1, 2.5, 2.7, 4.2, and 9.2×10^{-5} for intrinsic ACF coherence angle $\phi_c = 6'$, 12', 24', 36', 60', and 90', respectively.

As stated before, this is a conservative upper limit, making the assumption that all signal not attributed to the dust component is due to CBR anisotropy.

6. CONCLUSION

A search for the anisotropy of the CBR angular scales near 0°.5 has been described. The data contain contributions from the emission of ≈ 18 K Galactic dust and possibly another component. Fitting the data to two-component models including dust and 2.74 K Planck (CBR) emission yields a conservative upper limit to CBR fluctuations of $\Delta T/T \leq 2.5 \times 10^{-5}$ for a Gaussian ACF at an angular scale of 25'. If the second component were interpreted as due to CBR anisotropy, it would imply fluctuations with an rms of 45 μK (temperature difference for 2.74 K Planck spectrum), referred to the observing strategy described above. The measurement is an excellent test case for subtraction of foreground dust, identified by its spectrum and correlation with *IRAS*. Regions of the sky exist for which the expected anisotropic ISD emission is roughly a factor of 10 smaller than measured here. The measurement of dust structure at such a small level (10–50 μK) also demonstrates how far the system noise integrates down, and how well sidelobes, and a number of other potential systematic problems have been controlled.

In a previous experiment using the same telescope platform and a different detector (Meinhold & Lubin 1991), a Gaussian ACF upper limit of $\Delta T/T < 3.5 \times 10^{-5}$ was directly compared with various CDM models (Bond et al. 1991; Vittorio et al. 1991). To first order an upper limit a factor of 1.5 smaller than the previous one should force the biasing factor in the standard recombination model above 1.2, assuming $\Omega = 1$ and $\Omega_b = 0.05$. A detailed analysis will be presented in future publications.

The *COBE* DMR experiment has measured anisotropy at 10° at a level of $\Delta T/T = 1.1 \times 10^{-5}$. Normalized to this value, standard CDM models predict anisotropy at 30' to be roughly 50 μK (X. Gorski, private communication; J. R. Bond, private communication). This comparison depends on the details of the models, including reionization and baryon fraction. It should be noted that the measurements reported here sample a very small portion of the sky, and the limits set refer to *Gaussian* fluctuation models. If the distribution of fluctuations is not Gaussian, then measurements in some other region of the sky may well produce anisotropies above the limits quoted here for Gaussian ACF. Similar considerations apply to the recent upper limits of Gaier et al. (1992) at 1°.

This work was supported by the National Science Foundation through the Center for Particle Astrophysics (cooperative agreement AST-9120005), the National Aeronautics and Space Administration under grants NAGW-1062 and FD-NAGW-2121, the University of California, and previously by the California Space Institute. IPAC is funded by NASA as part of the *IRAS* extended mission program under contract to JPL. The authors would like to thank Jeffrey Schuster for useful discussions regarding telescope analysis and data analysis.

REFERENCES

Alsop, D. C., et al. 1992, ApJ, 317, 146
Bond, J. R., Efstathiou, G., Lubin, P. M., & Meinhold, P. R. 1991, Phys. Rev. Lett., 66, 2179
Devlin, M., et al. 1992, Proc. Nat. Acad. Sci., submitted
Fischer, M. L., et al. 1992, ApJ, 388, 242
Gaier, T., Schuster, J. A., Gundersen, J. O., Koch, T., Seiffert, M. D., Meinhold, P. R., & Lubin, P. M. 1992, ApJ, 398, L1
Gundersen, J. O., et al., 1993, in preparation
Meinhold, P. R., & Lubin, P. M. 1991, ApJ, 370, L11
Meinhold, P. R., et al. 1993, ApJ, 406, 612
Readhead, A. C. S., Lawrence, C. R., Myers, S. T., Sargent, W. L. W., Hardebeck, H. E., & Moffet, A. T. 1989, ApJ, 346, 566
Smoot, G. F., et al. 1992, ApJ, 396, L1
Sunyaev, R. A., & Zel'dovich, Ya. B. 1972, Comments Astrophys. Space Sci., 4, 173
Vittorio, N., Meinhold, P. R., Muciaccia, P. F., Lubin, P. M., & Silk, J. 1991, ApJ, 372, L1